

# Thermodynamic analysis of water vapor adsorption onto freeze-dried ora-pro-nobis (*Pereskia aculeata* Miller) mucilage

## Análise termodinâmica da adsorção de vapor de água em mucilagem de ora-pro-nóbis (*Pereskia aculeata* Miller)

Article Info:

Article history: Received 2023-06-05 / Accepted 2023-08-01 / Available online 2023-08-04

doi: 10.18540/jcecv19iss6pp16200-01e



**Bruna de Souza Nascimento**

ORCID: <https://orcid.org/0000000277978344>

Food Science Department, Federal University of Lavras, Brazil

E-mail: [bruna.nascimento@ufla.br](mailto:bruna.nascimento@ufla.br)

**Giovanni Aleixo Batista**

ORCID: <https://orcid.org/0000000212873074>

Food Science Department, Federal University of Lavras, Brazil

E-mail: [giovannialeixob@gmail.com](mailto:giovannialeixob@gmail.com)

**Vinicius Tessinari Pravato**

ORCID: <https://orcid.org/00000009000582526333>

Food Science Department, Federal University of Lavras, Brazil

E-mail: [vinicius.pravato@estudante.ufla.br](mailto:vinicius.pravato@estudante.ufla.br)

**Gabriel Pedroso de Lima Alexandre**

ORCID: <https://orcid.org/0000000191851182>

Food Science Department, Federal University of Lavras, Brazil

E-mail: [pedroso620@gmail.com](mailto:pedroso620@gmail.com)

**Lizzy Ayra Alcântara Veríssimo**

ORCID: <https://orcid.org/000000024860612X>

Food Science Department, Federal University of Lavras, Brazil

E-mail: [lizzy.alcantara@ufla.br](mailto:lizzy.alcantara@ufla.br)

**Jaime Vilela de Resende**

ORCID: <https://orcid.org/0000000228237304>

Food Science Department, Federal University of Lavras, Brazil

E-mail: [jvresende@ufla.br](mailto:jvresende@ufla.br)

### Resumo

A mucilagem de *Pereskia aculeata* Miller é um hidrocólide com potencial para ser utilizado como aditivo alimentar. Assim, obter informações a respeito de sua estabilidade física, química e microbiológica são necessários para avaliar a estabilidade de armazenamento do produto. Este estudo teve como objetivo determinar as propriedades termodinâmicas de adsorção de vapor de água em mucilagem de ora-pro-nóbis liofilizada (OPNM) e interpretar os mecanismos que governam a adsorção de água em partículas do pó através do estudo da compensação de entalpia-entropia. Além disso, OPNM foi caracterizado em termos de umidade, cinzas, extrato etéreo, proteínas, fibras e carboidratos bem como os grupos químicos funcionais por espectroscopia de infravermelho por transformada de Fourier (FTIR) e microscopia eletrônica de varredura (MEV). A análise termodinâmica mostrou que a adsorção de água no pó de OPNM foi caracterizada como um processo espontâneo com fortes forças atrativas na mistura água e OPNM. O mecanismo de sorção de água para OPNM na faixa de adsorção estudada foi regulado por interações energéticas relacionadas à composição química do produto.

**Palavras-chave:** Isotermas de adsorção. Modelo de GAB. Propriedades termodinâmicas. Fenômenos de sorção.

## Abstract

The mucilage of *Pereskia aculeata* Miller is a hydrocolloid with the potential to be used as a food additive. Thus, data on its physical, chemical and microbiological stability are necessary to evaluate the storage stability of the product. This study aimed to determine the thermodynamic properties of water vapor adsorption onto freeze-dried ora-pro-nobis mucilage (OPNM) and to interpret the mechanisms that govern water adsorption onto powder particles through the study of enthalpy-entropy compensation. In addition, OPNM was characterized in terms of moisture, ash, ether extract, protein, fiber and carbohydrates beyond the functional chemical groups by Fourier transform infrared spectroscopy (FTIR) and scanning electron microscopy (SEM). Thermodynamic analysis showed that water adsorption onto OPNM powder was characterized as a spontaneous process with strong attractive forces in the water and OPNM mixture. The water sorption mechanism for OPNM at the studied adsorption range was regulated by energy interactions related to the chemical composition of the product.

**Keywords:** Adsorption isotherms. GAB model. Thermodynamic properties. Sorption phenomenon.

## Nomenclature

$(\Delta S_{dif})_T$	Differential entropy [ $J mol^{-1} K^{-1}$ ]
$(H_v^0)_T$	Enthalpy of condensation of pure water [ $J mol^{-1}$ ].
$(H_v^0)_T$	Molar enthalpy of the condensation of pure water [ $J mol^{-1}$ ]
$(H_v^{dif})_T$	Total differential isosteric heat or total differential enthalpy of the adsorbed water [ $J mol^{-1}$ ]
$(H_v^{int})_T$	Total integral enthalpy of the water adsorbed onto the mucilage particles [ $J mol^{-1}$ ]
$(\Delta S_{int})_T$	Molar integral entropy [ $J mol^{-1} K^{-1}$ ]
$(\overline{\Delta H_{dif}})$	Mean differential enthalpy [ $J mol^{-1}$ ]
$(\overline{\Delta S_{dif}})$	Mean differential entropy [ $J mol^{-1} K^{-1}$ ]
$\Delta H_{dif}$	Differential molar enthalpy [ $J mol^{-1}$ ]
$A_m$	Surface area of a water molecule [ $1.06 \times 10^{-19} m^2$ ]
ATR	Attenuated total reflectance
$a_w$	Water activity [–]
BOD	Biological oxygen demand
C	Guggenheim constant [–]
C'	Integration constant [–]
FTIR	Fourier transform infrared spectroscopy.
GAB	Guggenheim-Anderson-de Boer
K	Constant correcting properties of the multilayer molecules with respect to the bulk liquid [–]
$K_B$	Boltzmann constant [ $1.38 \times 10^{-23} J m^2 s^{-2} K^{-1}$ ]
Meq	Equilibrium moisture content [% dry basis]
Mm	moisture content in the monolayer [% dry basis]
n	Number of temperatures evaluated [–]
$N_i$	Number of moles of water sorbed on the material surface [–]
$\emptyset$	Diffusion pressure or surface potential [ $J mol^{-1}$ ]
OPNM	Ora-pro-nobis mucilage
$P_v$	Water vapor pressure in the adsorbent [Pa]
$P_v^0$	Water vapor pressure at the same sorption temperature [Pa]
R	Universal ideal gas constant [ $8.314 J mol^{-1} K^{-1}$ ]
Rh	Relative air humidity
S	Total entropy of the sorbed state [ $J mol^{-1} K^{-1}$ ]
SEM	Scanning electron microscopy

$S_l$	Molar differential entropy [ $J mol^{-1} K^{-1}$ ]
$S_L$	Molar entropy of pure liquid water in equilibrium with vapor [ $J mol^{-1} K^{-1}$ ]
$S_s$	Molar integral entropy of water adsorbed onto the OPNM [ $J mol^{-1} K^{-1}$ ]
$T$	Temperatures used in the experiments [K]
$T_B$	Isokinetic temperature [K]
$T_{hm}$	Harmonic mean temperature [K]
$Var(T_B)$	Standard error of the isokinetic temperature [K]
$\Delta G$	Variation in Gibbs free energy [ $J mol^{-1}$ ]
$\Delta G_B$	Gibbs free energy associated with TB [ $J mol^{-1}$ ]

## 1. Introduction

*Pereskia aculeata* Miller, which is popularly known in Brazil as ora-pro-nobis, is a Cactaceae species with leaves rich in nontoxic mucilage with a high hydrocolloid content, consisting mainly of type I arabinogalactans, due to the covalent association of proteoglycans with proteins (Martin *et al.*, 2017). The chemical composition and technological properties of ora-pro-nobis mucilage (OPNM) are similar to those of gum arabic (Conceição *et al.*, 2014), making it a possible low-cost plant substitute for commercial gums.

The applications of OPNM include its use as stabilizer in the production of nanoemulsions (Lago *et al.*, 2019) and emulsified systems (Junqueira *et al.*, 2019), as a coating agent in biodegradable film for packaging (Oliveira *et al.*, 2019) and as a thickener and gelling agent for fermented dairy beverages (Amaral *et al.*, 2018). Because OPNM is a hydrocolloid with potential as a food additive, data are needed regarding its physical, chemical and microbiological stability, which is dependent on the water content and interactions with the constituents present (Amaral *et al.*, 2019; Conceição *et al.*, 2014; Junqueira *et al.*, 2019; Mrad *et al.*, 2012; Viganó *et al.*, 2012). Therefore, knowledge of the equilibrium relationship between the moisture content of the material and the relative humidity of the environment at different temperatures is of fundamental importance.

The sorption isotherms of OPNM at different temperatures allow the evaluation of the storage stability of the product and can be used in the design and control of the process (Mrad *et al.*, 2012). However, the complexity involved in transporting moisture through different materials means that several models proposed in the literature are used to correctly represent the sorption isotherms (Suppakul *et al.*, 2013). In addition, a thermodynamic approach to the adsorption process is also possible when there are sorption isotherms. This type of approach is useful for predicting the maximum stability conditions of food products beyond water activity and vitreous transition measurements (Silva *et al.*, 2014). It is possible to obtain a deep understanding of the sorption phenomenon and of the mechanism involved in the water vapor sorption process in different matrices (Azura and Beristain, 2006; Sánchez-Sáenz *et al.*, 2011).

The thermodynamic functions needed for an analysis of sorption behavior include Gibbs free energy, enthalpy and entropy (differential and integral functions). Gibbs free energy indicates the energy required for a molecule in the vapor state to change to the adsorbed state which is a quantitative measure of the affinity of water molecules for the surface of a solid and evinces the spontaneity of the adsorption process which is a quantitative measure of the affinity of water molecules for the surface of a solid (Bhattacharya *et al.*, 2008; Dotto *et al.*, 2013). The differential enthalpy of adsorption is a differential molar quantity derived from isotherm dependence and represents the binding energies of water molecules at a particular hydration level, while integral enthalpy is the average energy of all molecules already bound at a given level (Schneider, 1981). Changes in enthalpy values may be associated with water binding and repulsion forces with OPNM (Pérez-Alonso *et al.*, 2006). In addition, changes in entropy can define degrees of order or disorder existing in the water-OPNM system (Apostolopoulos and Gilbert, 1990), subjects not yet addressed in the OPNM literature.

In this context, the objective of this study was to characterize the freeze-dried OPNM in terms of its chemical composition and functional chemical groups by means of Fourier transform infrared spectroscopy (FTIR) and scanning electron microscopy (SEM). To determine the thermodynamic

properties of water vapor adsorption in freeze-dried OPNM and to interpret the mechanisms that governs the adsorption of water onto powder particles through the study of enthalpy-entropy compensation.

## 2. Materials and methods

### 2.1. Materials

Ora-pro-nobis branches were harvested at Federal University of Lavras, located in Lavras, Minas Gerais, Brazil. Undamaged leaves were separated from the stems, thorns and buds, cleaned and kept in a freezer at  $-20\text{ }^{\circ}\text{C}$  until the execution of the experiments.

### 2.2. Obtaining powdered OPNM

The extraction of OPNM was performed according to the method adapted from Lima Júnior *et al.* (2013). First, the ora-pro-nobis leaves were ground and homogenized in water at a ratio of 1 kg of ora-pro-nobis per 2.5 L of water, at  $100\text{ }^{\circ}\text{C}$  for 10 min, using an industrial blender (Metvisa, LG10). Then, the samples were placed in beakers and kept under stirring in a thermostatic bath (Quimis, q-215-2) at  $75\text{ }^{\circ}\text{C}$  for 6 h. The resulting homogenous material was filtered through organza cloth and subsequently subjected to vacuum filtration (Primar MC 1284, Brazil) using three layers of organza fabric as the filter. After filtration, the material was centrifuged at  $4680\text{ x g}$ . Ethanol was added to the remaining liquid at a 3:1 ratio (ethanol:solution). The precipitate, termed mucilage, was removed and frozen at  $-80\text{ }^{\circ}\text{C}$  and then lyophilized (Edwards, L4KR) at  $-40\text{ }^{\circ}\text{C}$  and 0.998 mbar for 120 h. The lyophilized material was then ground in a ball mill (SP Labor, SP-38) to obtain the powdered OPNM (Conceição *et al.*, 2014; Lima Junior *et al.*, 2013).

The lyophilized OPNM was hermetically packaged and stored in a desiccator at room temperature.

### 2.3. Proximate composition of OPNM

The OPNM was characterized in terms of moisture, ash, ether extract, protein, fiber and carbohydrates contents based on the Association of Official Analytical Chemists (AOAC, 2016). All analyses were performed in triplicate, and the results are expressed as the mean  $\pm$  standard deviation in percentage and dry weight.

### 2.4 FTIR spectroscopy and SEM

The FTIR spectrum of powdered OPNM was obtained by direct reading in the infrared region in a Varian 600-IR series FTIR spectrophotometer equipped with a GladiATR accessory (Pike Technologies) for attenuated total reflectance (ATR) measurements, at wavelengths between  $4000\text{ cm}^{-1}$  and  $500\text{ cm}^{-1}$ , with  $4\text{ cm}^{-1}$  resolution, using KBr pellets.

To evaluate the morphology of powdered OPNM, the samples were dried at  $70\text{ }^{\circ}\text{C}$  for 16 h and manually fixed to small stubs. Next, they were coated with a thin layer of gold and examined using a scanning electron microscope (LEO EVO 40 XVP, Zeiss, Cambridge, UK).

### 2.5 Determination of the equilibrium isotherms of OPNM

The equilibrium moisture contents of powdered OPNM were determined by the static gravimetric method using saturated saline solutions of LiCl,  $\text{MgCl}_2 \cdot 6\text{H}_2\text{O}$ ,  $\text{K}_2\text{CO}_3$ ,  $\text{Mg}(\text{NO}_3)_2 \cdot 6\text{H}_2\text{O}$ , NaCl, KCl and  $\text{K}_2\text{SO}_4$ , which correspond to a relative humidity range between 11% and 97% (Greenspan, 1977), and temperatures of 15, 25 and  $35\text{ }^{\circ}\text{C}$ .

Samples of OPNM weighing approximately 2 g were used for the moisture adsorption tests. To ensure a moisture of approximately zero, all samples were kept in a vacuum oven at  $70\text{ }^{\circ}\text{C}$  and 360 mmHg for 48 h. The different saline solutions were prepared in cylindrical glass jars, and the powders were placed in plastic containers located 4.0 cm from the base of the jars to avoid any contact between the liquid phase and the powders. To start the water sorption process, the jars were hermetically sealed and placed in a BOD incubator (Eletrolab, EL141) at controlled temperatures of 15, 25 and  $35\text{ }^{\circ}\text{C}$  and maintained under these conditions until reaching hygroscopic equilibrium.

The latter was determined when the sample showed constant weight in three consecutive weightings; in this case, constant weight was considered when the variations in the measurements were equal to 0.001 g. Upon reaching equilibrium, the dry weight of the samples was determined by the gravimetric method in an oven at 105 °C for 24 h. All experiments were performed in triplicate.

The relationship between the equilibrium moisture content (Meq) and the relative air humidity (Rh), which corresponds to the water activity (aw) of the OPNM at equilibrium, was predicted by the Guggenheim-Anderson-de Boer (GAB) model.

$$M_{eq} = \frac{M_m C K a_w}{(1 - K a_w)(1 - K a_w + C K a_w)} \quad (1)$$

where Meq is the equilibrium moisture content [% dry basis], aw is the water activity (dimensionless), Mm is the moisture content in the monolayer [% dry basis], C is the Guggenheim constant, and K is the constant correcting properties of the multilayer molecules with respect to the bulk liquid (Labuza *et al.*, 1985).

The GAB model parameters were estimated by nonlinear regression using the least squares method. The goodness-of-fit of the model was determined by the coefficient of determination (R<sup>2</sup>), the mean relative deviation modulus (E) and distribution of residuals.

## 2.6 Determination of thermodynamic properties

The Othmer method proposed by Beristain *et al.* (1994) was used to estimate OPNM differential and integral enthalpy and entropy. The aforementioned method considers the hypothesis that water adsorption happens in an inert solid, as the equilibrium is reached (between the water molecules adsorbed onto the solid and the surrounding molecules in the vapor state). The process occurs at low pressures and only water is adsorbed onto the surface of the solid (physisorption), thus the water vapor is considered an inert gas (Liébanes *et al.*, 2006).

### 2.6.1. Differential enthalpy and entropy

From the sorption equilibrium data using the Othmer equation (Othmer, 1940) the variations in the differential molar enthalpy ( $\Delta H_{dif}$ ) between water and OPNM were determined:

$$\frac{d \ln P_v}{d \ln P_v^0} = \frac{(H_v^{dif})_T}{(H_v^0)_T} \quad (2)$$

where the adsorbed substance is water vapor; Pv and Pv<sup>0</sup> represent the water vapor pressure in the adsorbent [Pa] and the water vapor pressure at the same sorption temperature [Pa], respectively; (Hv<sup>dif</sup>)<sub>T</sub> is the total differential isosteric heat or total differential enthalpy of the adsorbed water [J mol<sup>-1</sup>]; and (Hv<sup>0</sup>)<sub>T</sub> is the enthalpy of condensation of pure water [J mol<sup>-1</sup>].

If all terms in Equation (2) are dependent on temperature, Equation (3) is obtained from the integration of Equation (2) into constant moisture content (Meq).

$$\ln P_v = \left( \frac{(H_v^{dif})_T}{(H_v^0)_T} \right)_{M_{eq}} \ln (P_v^0) + C' \quad (3)$$

where C' is the integration constant.

In addition, if the relationship between (Hv<sup>dif</sup>)<sub>T</sub> and (Hv<sup>0</sup>)<sub>T</sub> remains constant in the evaluated temperature range, a graph of ln(Pv) versus ln(Pv<sup>0</sup>) will result in a straight line (Silva *et al.*, 2014). Therefore, the (Hv<sup>dif</sup>)<sub>T</sub>/(Hv<sup>0</sup>)<sub>T</sub> ratio is obtained from the slope of the line obtained by linear

regression and the differential isosteric heat or differential enthalpy  $(\Delta H_{dif})_T$  is defined by Equation (4):

$$(-\Delta H_{dif})_T = \left( \frac{(H_v^{dif})_T}{(H_v^0)_T} - 1 \right)_{Meq} (H_v^0)_T \quad (4)$$

To obtain the enthalpy of condensation of pure water values as a function of the evaluated temperature  $((H_v^0)_T$ , in  $[J \text{ mol}^{-1}]$ ), Equation (5) proposed by Wexler (1976) and was used by Greenspan (1977). By replacing the values of  $(H_v^{dif})_T/(H_v^0)_T$  and  $(H_v^0)_T$  in Equation (4), it is possible to obtain the differential enthalpy  $(\Delta H_{dif})$  of adsorption at different temperatures.

$$(H_v^0)_T = 6.17 \times 10^4 - 94.18 \times T + 17.76 \times 10^{-2} T^2 - 2.04 \times 10^{-4} T^3 \quad (5)$$

For the differential entropy  $(\Delta S_{dif})_T$ , the values were determined by the Gibbs-Helmholtz equation (Equation 6):

$$\Delta G = (\Delta H_{dif})_T - T(\Delta S_{dif})_T \quad (6)$$

where  $\Delta G$  corresponds to the variation in Gibbs free energy, calculated by Equation (7) (Iglesias *et al.*, 1976):

$$\Delta G = RT \ln(a_w) \quad (7)$$

$\Delta G$  is a function of the absolute temperature  $T$  [K],  $a_w$  is the dimensionless parameter that represents water activity, and  $R$  is the universal ideal gas constant  $[8.314 \text{ J mol}^{-1} \text{ K}^{-1}]$ .

Substituting the Gibbs-Helmholtz equation (Equation 6) and the values of  $(\Delta H_{dif})_T$  calculated by Equation (4) in Equation (8), it is possible to estimate the differential entropy values  $(\Delta S_{dif})_T$ :

$$(\Delta S_{dif})_T = S_l - S_l = -\frac{(\Delta H_{dif})_T}{T} - R \ln(a_w) \quad (8)$$

in this case,  $S_l = (\partial S / \partial N_l)_T$ ,  $P$  is the molar differential entropy of the water in the sorbed state  $[J \text{ mol}^{-1} \text{ K}^{-1}]$ ,  $S_L$  is the molar entropy of pure liquid water in equilibrium with vapor  $[J \text{ mol}^{-1} \text{ K}^{-1}]$ ,  $S$  is the total entropy of the sorbed state  $[J \text{ mol}^{-1} \text{ K}^{-1}]$ , and  $N_l$  is the number of moles of water sorbed on the material surface.

### 2.6.2. Integral enthalpy and entropy

For the determination of the integral thermodynamic properties of OPNM, the calculations followed a procedure similar to that of the differential properties; however, constant diffusion pressure ( $\Phi$ ) is used rather than equilibrium moisture (Meq).

$$(-\Delta H_{int})_T = \left( \frac{(H_v^{int})_T}{(H_v^0)_T} - 1 \right)_{\Phi} (H_v^0)_T \quad (9)$$

where  $(H_v^{int})_T$  is the total integral enthalpy of the water adsorbed onto the mucilage particles  $[J \text{ mol}^{-1}]$  and  $(H_v^0)_T$  is the molar enthalpy of the condensation of pure water  $[J \text{ mol}^{-1}]$ .

The diffusion pressure ( $\Phi$ ) was estimated by Equation (10) as described by Iglesias *et al.* (1976) and Al-Mutusaeb *et al.* (2004).

$$\phi = \frac{K_B T}{A_m} \int_0^{a_w} \frac{M_{eq}}{M_m a_w} da_w \quad (10)$$

where ( $\phi$ ) is the diffusion pressure or surface potential [ $\text{J mol}^{-1}$ ],  $K_B$  is the Boltzmann constant [ $1.38 \times 10^{-23} \text{ J m}^2 \text{ s}^{-2} \text{ K}^{-1}$ ] and  $A_m$  is the surface area of a water molecule [ $1.06 \times 10^{-19} \text{ m}^2$ ].

Substituting the GAB equation (Equation 1) into Equation (10) and performing the necessary analytical development, a mathematical definition for the constant diffusion pressure ( $\phi$ ) is obtained, given by Equation (11):

$$\phi = \frac{K_B T}{A_m} \ln \left( \frac{1 - k a_w + C k a_w}{1 - k a_w} \right) \quad (11)$$

The  $(\Delta H_{int})_T$  values calculated by Equation (9) are used to calculate the variation in the molar integral entropy  $(\Delta S_{int})_T$  given by Equation (12), similar to that calculated for  $(\Delta S_{dif})_T$ .

$$(\Delta S_{int})_T = S_s - S_L = -\frac{(\Delta H_{int})_T}{T} - R \ln(a_w) \quad (12)$$

in this case  $S_s = (S/N)$  is the molar integral entropy of water adsorbed onto the OPNM [ $\text{J mol}^{-1} \text{ K}^{-1}$ ] and  $S_L$  is the molar entropy of the condensation of pure water [ $\text{J mol}^{-1} \text{ K}^{-1}$ ].

### 2.6.3 Enthalpy-entropy compensation theory

The physical phenomenon characterized during the adsorption process was determined by enthalpy-entropy compensation theory or isokinetic compensation theory, which proposes the existence of a linear relationship between the enthalpy and entropy of water adsorption (Beristain *et al.*, 1996), as shown in Equation (13).

$$(\Delta H_{dif})_T = T_B (\Delta S_{dif})_T + \Delta G_B \quad (13)$$

where  $T_B$  is the isokinetic temperature [K], which represents the temperature at which all reactions during adsorption occur at the same rate; and  $\Delta G_B$  [ $\text{J mol}^{-1}$ ] is the Gibbs free energy associated with  $T_B$ .

To validate the compensation theory, the isokinetic temperature ( $T_B$ ) value obtained from the linear relationship between the enthalpy and entropy of adsorption was compared with the harmonic mean temperature [K], Equation (14), which represents the mean of the temperatures ( $T$ ) used in the experiments (Krug *et al.*, 1976).

$$T_{hm} = \frac{n}{\sum_{i=1}^n \left( \frac{1}{T} \right)} \quad (14)$$

where  $T$  represents the temperatures used in the experiments and  $n$  is the number of temperatures evaluated.

According to Krug *et al.* (1976) the compensation theory is only applied if  $T_B \neq T_{hm}$ . If  $T_B > T_{hm}$ , the adsorption phenomenon is controlled by enthalpy, whereas if  $T_B < T_{hm}$ , it is controlled by entropy.

The confidence interval,  $(1-\alpha)100\%$ , for the isokinetic temperature ( $T_B$ ) is given by:

$$T_B = T_B \pm t_{m-2, \alpha/2} \sqrt{\text{Var}(T_B)} \quad (15)$$

$$\text{Var}(T_B) = \frac{\sum_{i=1}^n [(\Delta H_{dif})_T - (\overline{\Delta H}_{dif})_T] [(\Delta S_{dif})_T - (\overline{\Delta S}_{dif})_T]}{(m-2) \sum_{i=1}^n [(\Delta S_{int})_T - (\overline{\Delta S}_{int})_T]^2} \quad (16)$$

in this case  $T_B$ : slope inclination of the enthalpy-entropy compensation with a confidence interval of 95% calculated for all data sets;  $m$ : number of data pairs ( $\Delta H_{dif}$ ,  $\Delta S_{dif}$ );  $(\overline{\Delta H}_{dif})$ : mean differential enthalpy;  $(\overline{\Delta S}_{dif})$ : mean differential entropy;  $\text{Var}(T_B)$ : standard error of the isokinetic temperature.

### 3. Results and discussion

#### 3.1 Proximate composition of OPNM

The proximate composition on a dry basis of OPNM was  $9.38 \pm 0.08\%$  moisture,  $0.57 \pm 0.02\%$  ether extract,  $14.24 \pm 0.03\%$  protein,  $2.45 \pm 0.29\%$  fiber,  $10.03 \pm 0.04\%$  ash and  $63.36 \pm 0.21\%$  carbohydrate.

The protein and carbohydrate contents obtained in this study were higher than the values of 10.47% and 46.88% reported by Lima Junior *et al.* (2013) for mucilage obtained from ora-pro-nobis leaves and lower than the protein content of 28.4% reported by Takeite *et al.* (2009) for fresh ora-pro-nobis leaves. These differences are attributed to external factors such as climatic changes, soil nutrition and preprocessing methods. For instance, Lima Júnior *et al.* (2013) froze the leaves and stored them under refrigeration before processing.

#### 3.2 Chemical and morphological characterization of OPNM

The FTIR spectrum of OPNM (Figure 1) showed characteristic bands at  $3393 \text{ cm}^{-1}$  attributed to the O–H stretching of cellulose. A band at  $2930 \text{ cm}^{-1}$  was also observed, corresponding to the asymmetric deformation of  $-\text{C}-\text{H}$  ( $\text{sp}^3$ ), a peak at  $1640 \text{ cm}^{-1}$  attributed to the bond of the starch group ( $-\text{N}-\text{H}$ ), and a band at  $1330 \text{ cm}^{-1}$ , which is attributed to  $-\text{CH}$  stretching vibrations. The spectral bands and peaks are characteristic of glycoproteins such as arabinogalactan (Conceição *et al.*, 2014; Lima Junior *et al.*, 2013).

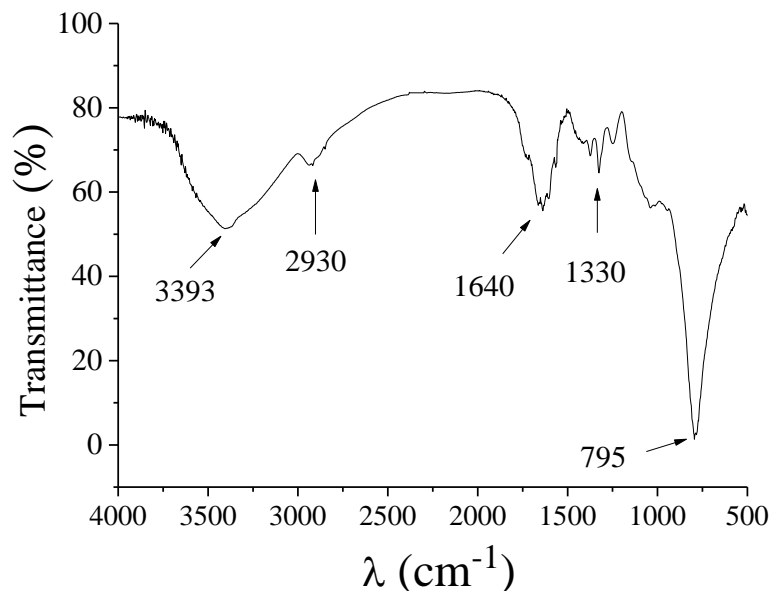


**Figure 1 - FTIR spectrum of lyophilized OPNM.**

Similarities were found between the spectral bands for OPNM obtained in this study and those found by Mercê *et al.* (2000) and Conceição *et al.* (2014) for OPNM, with differences only in the intensity of the bands. Those authors also report the existence of a twist in the main chain of a biopolymer containing linked rhamnose units (1/2).

Figure 2 shows the SEM image (1000x magnification) of the OPNM powder, revealing an amorphous, heterogeneous, granular structure with clusters of variable sizes.

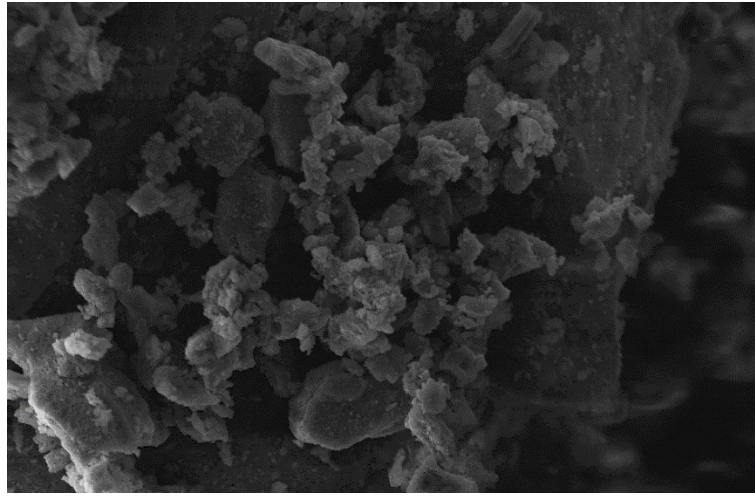


**Figure 2 - SEM image of OPNM powder (1000x magnification).**

### 3.3. Adsorption isotherm of OPNM

The variation in the equilibrium moisture content (Meq) as a function of the water activity ( $a_w$ ) of the OPNM powder, as well as the fit of the GAB model at the temperatures of 15, 25 and 35 °C, are shown in Figure 3. The adsorption isotherms have a shape characteristic of type II isotherms, based on the Brunauer classification (Al-Muhtased *et al.*, 2002), similar to most water adsorption isotherms of biopolymers such as gum arabic, mesquite gum (Pérez-Alonso *et al.*, 2006) and chia seed mucilage (Velázquez-Gutiérrez *et al.*, 2015).

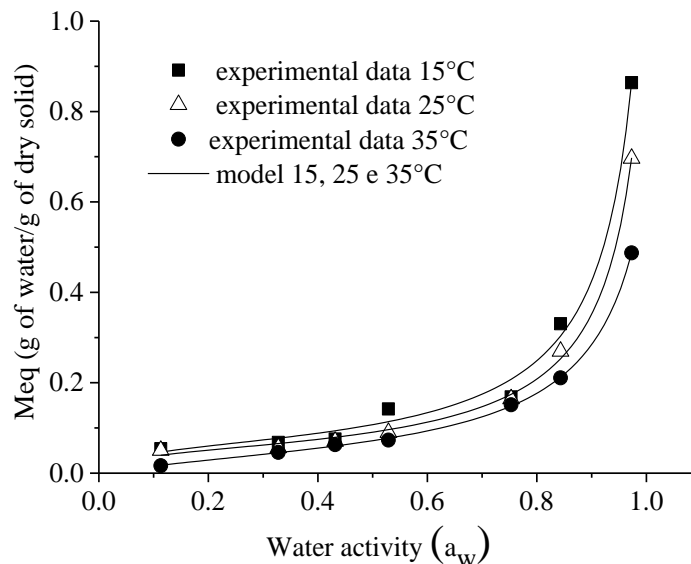


**Figure 3 - Adsorption isotherms of lyophilized OPNM at temperatures of 15, 25 and 35 °C.**

The experimental data presented in Figure 3 show that for a given  $a_w$ , Meq decreases with increasing temperature because the water molecules increase the energy level, becoming unstable.

As the temperature increases, the intermolecular interactions between the water molecules and the adsorption sites are broken (McMinn and Magee, 2003).

Physical and chemical changes caused by temperature resulted in a decrease in the total number of active water-binding sites. Thus, mobility of water molecules and the adsorbed phase/vapor phase dynamic equilibrium are affected (Goula *et al.*, 2008). Temperature influence on the sorption isotherms plays an important role regarding the acceleration of chemical and biological reactions during the processing and storage of a product (Lago and Noreña, 2015; Moreira *et al.*, 2008).

The  $M_m$ ,  $C$  and  $K$  parameters of the GAB model are listed in Table 1. For all evaluated temperatures, the  $R^2$  values found were close to one, and the  $E$  was less than 10%, demonstrating a good fit of the GAB model to the experimental data. According to Liébanes *et al.* (2006), the theory described by the GAB model indicates that the water monolayer located on the solid surface is strongly limited, while the water molecules in the multilayers are less attracted to the solid. Water molecules that are not affected by the presence of the solid are described as free water molecules.

**Table 1 - GAB model parameters estimated by nonlinear regression.**

T (°C)	$M_m$ [g H <sub>2</sub> O/g dry solid]	C	K	$R^2$	E [%]
15	0.059	19.433	0.958	0.997	2.857
25	0.050	19.717	0.954	0.999	2.190
35	0.050	3.910	0.925	0.999	1.142

Based on the results presented in Table 1, the water content in the monolayer ( $M_m$ ) ranged from 0.059 to 0.050 [g of H<sub>2</sub>O/g of dry solid]. This parameter represents the ideal moisture content to be obtained during the storage of a material to ensure product stability and minimize undesirable biological and chemical reactions (Pérez-Alonso *et al.*, 2006). Parameter  $C$ , which indicates the binding energy of water adsorption in the monolayer, presented a lower value at 35 °C, showing easier breaking of the monolayer bonds. Subsequently, relatively weak bonds present in the adjacent multilayers are broken, causing greater deterioration of the material (Monte *et al.*, 2018). The  $k$  values were close to one, which demonstrates the pure state of the adsorbent in the multilayers. This result shows that when the OPNM is subjected to a certain  $a_w$  and temperature, its water molecules will have the physical properties of pure water in the free state.

#### 3.4. Differential enthalpy and entropy

Figure 4 shows the results for the variation in differential enthalpy ( $-\Delta H_{dif}$ ) and entropy ( $\Delta S_{dif}$ ) as a function of the equilibrium moisture content in OPNM at 25 °C. Both parameters are strongly dependent on the moisture content of OPNM.

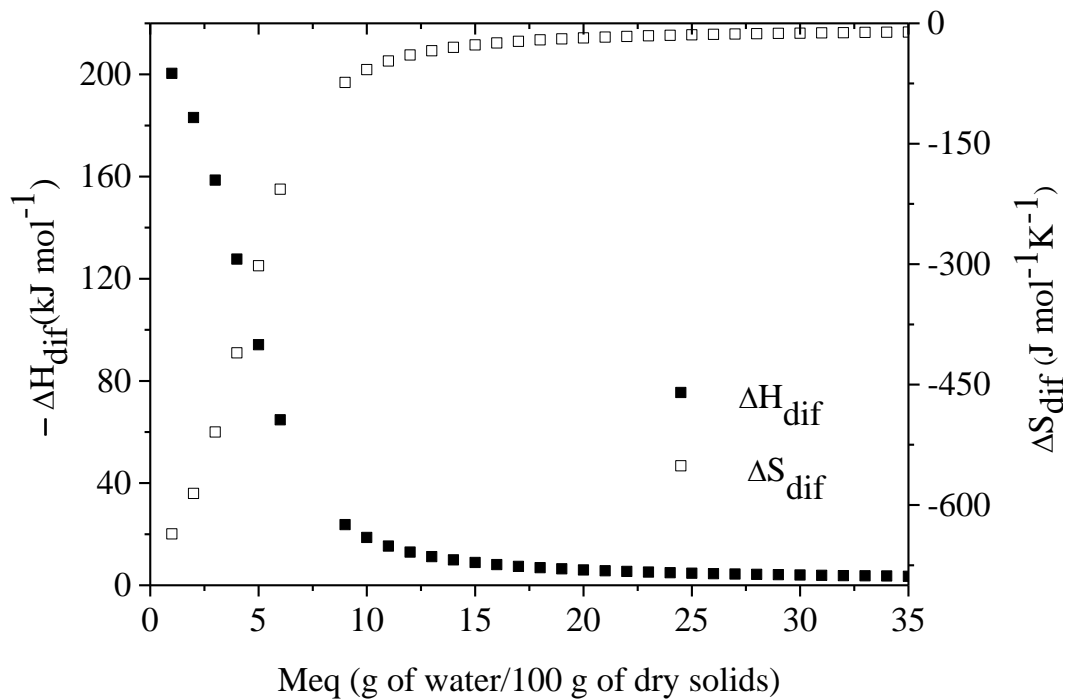


**Figure 4 - Variation in differential enthalpy and entropy for water adsorption in the OPNM at 25 °C.**

For differential enthalpy  $\Delta H_{\text{dif}}$ , the existence of strong attractive forces in the water/OPNM mixture is suggested by the results, once all values were negative (Pérez-Alonso *et al.*, 2006). Pérez-Alonso *et al.* (2006) reported the same behavior for different biopolymers of pure and mixed carbohydrates, such as gum arabic, maltodextrin and mesquite gum.

The highest ( $-\Delta H_{\text{dif}}$ ) value found was approximately  $200 \text{ kJ mol}^{-1}$ , when the moisture content was close to 0.00 [g water/g dry OPNM], which is considerably far from the moisture content value in the monolayer (Mm), equal to 0.05 [g of H<sub>2</sub>O/g of dry solid] (Table 1). According to Liébanes *et al.* (2006), this behavior occurs because there are energetically different adsorption sites on the solid surface, and high ( $-\Delta H_{\text{dif}}$ ) values indicate a greater solid-water interaction. When the Meq values increase, the solid-water interaction becomes weaker, and multilayers form; consequently, lower ( $-\Delta H_{\text{dif}}$ ) values are observed (Liébanes *et al.*, 2006; McMinn and Magee, 2003). The same trend was observed by Pérez-Alonso *et al.* (2006) for maltodextrin under experimental conditions similar to those evaluated in this study.

The differential enthalpy values for OPNM tended to be constant and close to zero (Figure 4), indicating that the heat of sorption value was close to the heat of water vaporization one. The moisture content corresponding to a heat of sorption close to the enthalpy of vaporization of pure water is often used as a limiting indicator of the water content present in food (Tunç and Duman, 2007). However, changes in the heat of vaporization with the moisture content provide important data for understanding the interaction between solid-water and water-water, in addition to determining the energy consumed in a process and being used in the dimensioning of equipment (McMinn and Magee, 2003).

For differential entropy, a continuous increase until a moisture content of 15 [g of water/100 g of dry solid] was observed, remaining practically constant at higher moisture contents (Figure 4). Differential entropy is defined as the sum of integral entropy at a certain level of hydration and the

change in order or disorder after the system absorbs the new water molecules at the same level of hydration (Pérez-Alonso *et al.*, 2006). If the minimum differential entropy and the minimum integral entropy moisture values are different, it is not possible to consider this special hydration level at the minimum differential entropy the point of maximum stability, since not all accessible active sites were occupied in that specific amount of water. Consequently, after this point, smaller differential changes that promote an improvement in the ordering of the water molecules adsorbed onto the food may be obtained. Thus, the water content at the minimum differential entropy was comparable to the GAB monolayer values, which correspond to the water adsorbed onto the most active sites, due to water sorption onto the most active sites caused the maximum change in entropy. The same trend in differential entropy versus moisture content was found by Pérez-Alonso *et al.* (2006) for maltodextrin under the same conditions evaluated here.

### 3.5. Gibbs free energy

Figure 5 shows the results obtained for the calculation of the Gibbs free energy variation as a function of the OPNM equilibrium moisture content at 15, 25 and 35 °C. This property is a quantitative measure of the affinity of water for the surface of a solid, i.e.,  $\Delta G$  provides information about the amount of free energy required to transfer a molecule in the vapor state to a solid surface (Iglesias *et al.*, 1976). In addition, it is used as a criterion of the spontaneity ( $-\Delta G$ ) or non-spontaneity ( $+\Delta G$ ) of the adsorption process (Bhattacharya *et al.*, 2008).

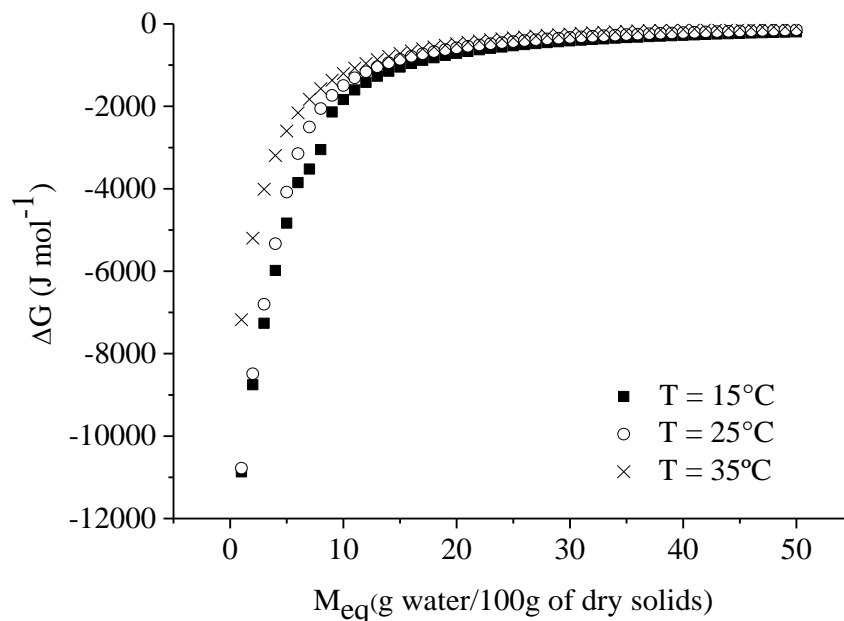


**Figure 5 - Variation in Gibbs free energy as a function of the equilibrium moisture content for OPNM.**

The results presented in Figure 5 show that for all temperatures, the  $\Delta G$  values calculated by Equation 7 increase exponentially with the increase in  $M_{eq}$  until reaching a constant value, close to zero. In addition, negative  $\Delta G$  values are observed for all evaluated experimental conditions, demonstrating that water adsorption in powdered OPNM is a spontaneous process. The more negative the  $\Delta G$  value is, the more spontaneous and energetically favorable the process is, as observed for lower  $M_{eq}$  values (Figure 5).

For the highest  $M_{eq}$  levels, adsorption occurs with less spontaneity because under this condition, the interaction forces between the matrix and adsorbent decrease due to the probable formation of multilayers of water molecules (Silva *et al.*, 2014). The results found in this study are

in agreement with those reported by Pérez-Alonso *et al.* (2006) for gum arabic, maltodextrin and mesquite gum, used pure and as blends.

### 3.6. Integral enthalpy and entropy

Integral enthalpy is a parameter that measures the average energy of all water molecules already bound to the adsorbent surface at a given moisture content (Bonilla *et al.*, 2010) and can be interpreted as transition enthalpy or phase change enthalpy, providing information about the energy changes required for the sorption process (Viganó *et al.*, 2012). As shown in Figure 6, the integral enthalpy of powdered OPNM decreased with increasing moisture content, a behavior similar to that found for potato starch (Al-Muhtaseb *et al.*, 2004), dehydrated yacon bagasse (Lago and Noreña, 2015) and maltodextrin (Pérez-Alonso *et al.*, 2006).

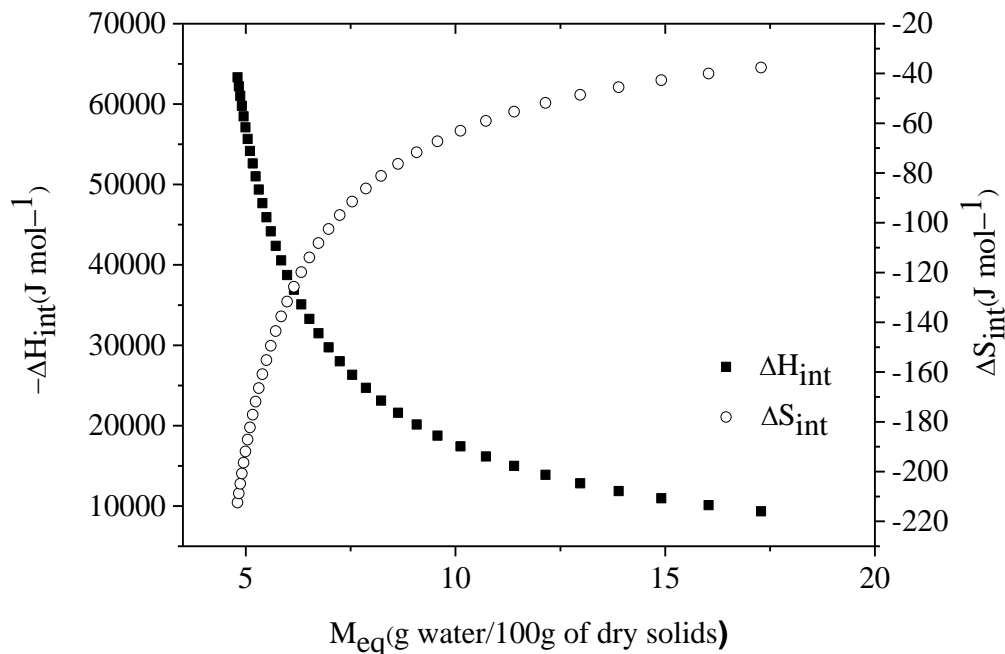


**Figure 6 - Variation in differential enthalpy and entropy for water adsorption onto OPNM.**

According to McMinn and Magee (2003), high energy requirements at low moisture levels indicate the presence of polar sites on the surface of a material, resulting in the lower mobility of water molecules. For the maximum integral enthalpy value ( $63.32 \text{ kJ mol}^{-1}$ ), there is coverage of the strongest binding sites and greater water-solid interaction (Fasina, 2006). Another important finding is that the moisture at which the maximum integral enthalpy is reached is close to the moisture value of the monolayer obtained in the GAB model. This result is consistent because  $M_m$  (water content in the monolayer) indicates the amount of water that is strongly adsorbed in specific locations, and to break these bonds, a larger amount of energy is needed than for other moisture contents (Silva *et al.*, 2014).

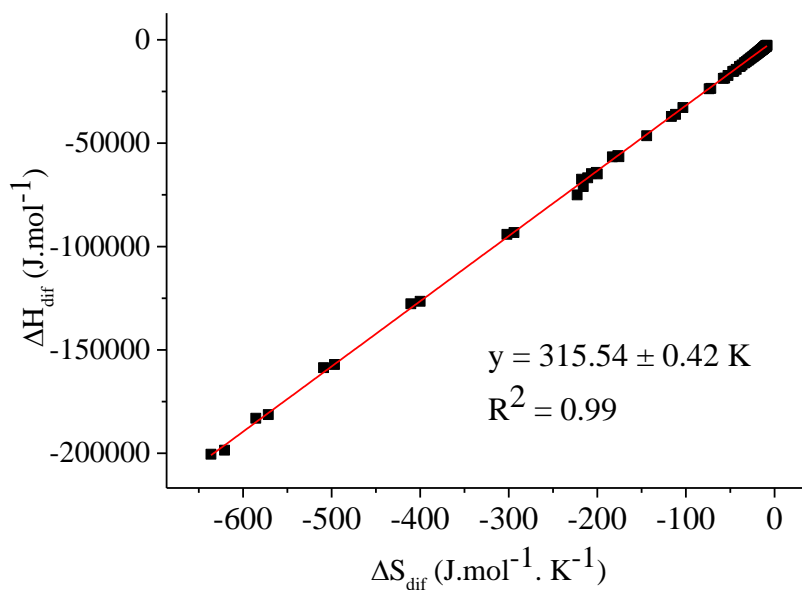
The coverage of less favorable sites and the formation of multiple layers of adsorbed water are mentioned as the main reasons for the decrease in integral enthalpy with increasing moisture content (Kaya and Kahyaoglu, 2007). The increase in moisture content causes the adsorbent sites to become saturated, and the water molecules are retained from the particles due to the difference in surface tension by a chemical adsorption process (Aviara *et al.*, 2004). In this case, as the surface tension forces are weaker and breakable, less energy is required; therefore, lower integral enthalpy values are observed.

Figure 6 also shows the results for net integral entropy. At low moisture contents, the integral entropy presented the lowest result, and with the increase in moisture content, the entropy values

increased continuously (Figure 6), as observed for potato starch (McMinn *et al.*, 2004), yacon bagasse (Lago and Noreña, 2015) and maltodextrin (Pérez-Alonso *et al.*, 2006). The net integral entropy can be interpreted qualitatively or quantitatively in terms of the order-disorder of the adsorbed molecules (Rizvi and Benado, 1983). In our study, entropy showed lower values at lower moisture contents and increased rapidly as the water covered the surface-forming layers. Rizvi and Benado (Rizvi and Benado, 1983) reported that in food, two opposite entropic contributions after moisture adsorption are possible: an entropy loss because of the location of water and increased entropy due to the structural transformation resulting from the change in volume and solubilization. The presence of chemical adsorption and/or changes in the adsorbent structure resulted in the negative values found (Iglesias *et al.*, 1976). Equal tendency is found in the literature for yacon bagasse (Lago and Noreña, 2015) and maltodextrin (Pérez-Alonso *et al.*, 2006).

### 3.7. Compensation theory

The relationship of differential enthalpy as a function of differential entropy of OPNM is shown in Figure 7, providing evidence of the existence of a linear relationship between them, with  $R^2 = 0.99$ . Thus, compensation theory can be applied to evaluate the adsorption process under the conditions used here. Notably, both differential enthalpy and entropy were considered independent of temperature at a moisture level.



**Figure 7 - Relationship of differential enthalpy and entropy for water adsorption in OPNM.**

Figure 7 shows that the isokinetic temperature ( $T_B$ ) was  $315,54 \pm 0.42$  K, which is significantly different from  $T_{hm} = 297.92$  K at a 95% confidence level. Therefore, the application of isokinetic compensation theory has been confirmed. Thus, the water adsorption process for OPNM was enthalpically directed because  $T_B > T_{hm}$ , that is, energy interactions related to the chemical composition of the product regulated the water sorption mechanism for OPNM at the studied temperature range (Beristain *et al.*, 1996).

### 3. Conclusions

The proximate composition on a dry basis of OPNM was  $9.38 \pm 0.08\%$  moisture,  $0.57 \pm 0.02\%$  ether extract,  $14.24 \pm 0.03\%$  protein,  $2.45 \pm 0.29\%$  fiber,  $10.03 \pm 0.04\%$  ash and  $63.36 \pm 0.21\%$  carbohydrate. The spectral bands and peaks are characteristic of glycoproteins such as

arabinogalactan. The SEM images of the OPNM showed an amorphous, heterogeneous, granular structure with clusters of variable sizes.

The adsorption isotherms showed a shape characteristic of type II isotherms, and the GAB model showed good fit to the experimental data at the three evaluated temperatures (15, 25 and 35 °C); the model was used to calculate the thermodynamic properties with spontaneous representation of the process of water adsorption onto OPNM.

Through thermodynamic analysis, it was possible to obtain important information related to the mechanisms that control the water adsorption process of powdered OPNM; the mechanism is characterized as a spontaneous process with strong attractive forces in the water and OPNM mixture.

The isokinetic compensation theory was confirmed, with an isokinetic temperature ( $T_B$ ) of  $315.54 \pm 0.42$  K, which is higher and significantly different from  $T_{hm} = 297.92$  K at a 95% confidence level. Thus, the water adsorption process of OPNM was enthalpically directed. Therefore, energy interactions related to the chemical composition of the product regulated the water sorption mechanism for OPNM at the studied temperature range.

### Acknowledgments

The authors thank the Center of Analysis and Chemical Prospecting of the Federal University of Lavras for supplying the equipment and technical support for experiments involving FTIR analyses, Coordination for the Improvement of Higher Education Personnel (CAPES), the Foundation for Research Support of Minas Gerais (FAPEMIG – APQ-00795-22 and APQ-02339-21) and the National Council for Scientific and Technological Development (CNPQ).

### References

- Al-Muhtaseb, A. H., McMinn, W. A. M., & Magee, T. R. A. (2004). Water sorption isotherms of starch powders. Part II: Thermodynamic characteristics. *Journal of Food Engineering*, 62(2), 135–142. [https://doi.org/10.1016/S0260-8774\(03\)00202-4](https://doi.org/10.1016/S0260-8774(03)00202-4)
- Al-Muhtased, A. H., McMinn, W. A. M., & Magee, T. R. A. (2002). Moisture sorption isotherm characteristics of food products: A review. *Food and Bioproducts Processing: Transactions of the Institution of Chemical Engineers, Part C*, 80(2), 118–128. <https://doi.org/10.1205/09603080252938753>
- Amaral, T. N., Junqueira, L. A., Prado, M. E. T., Cirillo, M. A., de Abreu, L. R., Costa, F. F., & de Resende, J. V. (2018). Blends of *Pereskia aculeata* Miller mucilage, guar gum, and gum Arabic added to fermented milk beverages. *Food Hydrocolloids*, 79, 331–342. <https://doi.org/10.1016/j.foodhyd.2018.01.009>
- Amaral, T. N., Junqueira, L. A., Tavares, L. S., Oliveira, N. L., Prado, M. E. T., & Resende, J. V. de. (2019). Effects of salts and sucrose on the rheological behavior, thermal stability, and molecular structure of the *Pereskia aculeata* Miller mucilage. *International Journal of Biological Macromolecules*, 131, 218–229. <https://doi.org/10.1016/j.ijbiomac.2019.03.063>
- AOAC. (2016). Official methods of analysis of AOAC international: Vols. I–II (G. W. Latimer Jr., Org.; 20<sup>o</sup> ed). AOAC International.
- Apostolopoulos, D., & Gilbert, S. G. (1990). Water sorption of coffee solubles by frontal inverse gas chromatography: Thermodynamic considerations. *Journal of Food Science*, 55(2), 475–487. <https://doi.org/10.1111/j.1365-2621.1990.tb06790.x>
- Aviara, N. A., Ajibola, O. O., & Oni, S. A. (2004). Sorption Equilibrium and Thermodynamic Characteristics of Soya Bean. *Biosystems Engineering*. <https://doi.org/10.1016/j.biosystemseng.2003.11.006>
- Azuara, E., & Beristain, C. I. (2006). Enthalpic and entropic mechanisms related to water sorption of yogurt. *Drying Technology*, 24(11), 1501–1507. <https://doi.org/10.1080/07373930600961173>

- Beristain, C. I., Diaz, R., Azuara, E., & Garcia, H. S. (1994). Thermodynamic behavior of green whole and decaffeinated coffee beans during adsorption. *Em Drying Technology* (Vol. 12, Número 5, p. 1221–1233). <https://doi.org/10.1080/07373939408960997>
- Beristain, C. I., Garcia, H. S., & Azuara, E. (1996). Enthalpy-Entropy compensation in food vapor adsorption. *Journal of Food Engineering*. [https://doi.org/10.1016/s0260-8774\(96\)00011-8](https://doi.org/10.1016/s0260-8774(96)00011-8)
- Bhattacharya, A. K., Naiya, T. K., Mandal, S. N., & Das, S. K. (2008). Adsorption, kinetics and equilibrium studies on removal of Cr(VI) from aqueous solutions using different low-cost adsorbents. *Chemical Engineering Journal*, 137(3), 529–541. <https://doi.org/10.1016/j.cej.2007.05.021>
- Bonilla, E., Azuara, E., Beristain, C. I., & Vernon-Carter, E. J. (2010). Predicting suitable storage conditions for spray-dried microcapsules formed with different biopolymer matrices. *Food Hydrocolloids*, 24(6–7), 633–640. <https://doi.org/10.1016/j.foodhyd.2010.02.010>
- Conceição, M. C., Junqueira, L. A., Cristina, K., Silva, G., Elisabeth, M., Prado, T., & Resende, J. V. De. (2014). Food Hydrocolloids Thermal and microstructural stability of a powdered gum derived from *Pereskia aculeata* Miller leaves. *Food hydrocolloids*, 40, 104–114. <https://doi.org/10.1016/j.foodhyd.2014.02.015>
- Dotto, G. L., Moura, J. M., Cadaval, T. R. S., & Pinto, L. A. A. (2013). Application of chitosan films for the removal of food dyes from aqueous solutions by adsorption. *Chemical Engineering Journal*, 214, 8–16. <https://doi.org/10.1016/j.cej.2012.10.027>
- Fasina, O. O. (2006). Thermodynamic properties of sweetpotato. *Journal of Food Engineering*, 75(2), 149–155. <https://doi.org/10.1016/j.jfoodeng.2005.04.004>
- Goula, A. M., Karapantsios, T. D., Achilias, D. S., & Adamopoulos, K. G. (2008). Water sorption isotherms and glass transition temperature of spray dried tomato pulp. *Journal of Food Engineering*. <https://doi.org/10.1016/j.jfoodeng.2007.07.015>
- Greenspan, L. (1977). Humidity fixed points of binary saturated aqueous solutions. *Journal of Research of the National Bureau of Standards. Section A, Physics and Chemistry*, 81A(1), 89. <https://doi.org/10.6028/JRES.081A.011>
- Iglesias, H. A., Chirife, J., & Viollaz, P. (1976). Thermodynamics of water vapour sorption by sugar beet root. 11, 91–101.
- Junqueira, L. A., Amaral, T. N., Félix, P. C., Botrel, D. A., Prado, M. E. T., & Resende, J. V. de. (2019). Effects of change in PH and addition of sucrose and NaCl on the emulsifying properties of mucilage obtained from *Pereskia aculeata* Miller. *Food and Bioprocess Technology*, 12(3), 486–498. <https://doi.org/10.1007/s11947-018-2223-1>
- Kaya, S., & Kahyaoglu, T. (2007). Moisture sorption and thermodynamic properties of safflower petals and tarragon. *Journal of Food Engineering*, 78(2), 413–421. <https://doi.org/10.1016/j.jfoodeng.2005.10.009>
- Krug, R. R., Hunter, W. G., & Grieger, R. A. (1976). Enthalpy-entropy compensation. 2. Separation of the chemical from the statistical effect. *The Journal of Physical Chemistry*, 80(21), 2341–2351. <https://doi.org/10.1021/j100562a007>
- Labuza, T.P.; Kaanane, A.; Chein, J. Y. (1985). Effect of temperature on the moisture sorption isotherms and water activity shift of two dehydrated food. *Journal of Food Science*, 50, 385–391.
- Lago, A. M. T., Neves, I. C. O., Oliveira, N. L., Botrel, D. A., Minim, L. A., & de Resende, J. V. (2019). Ultrasound-assisted oil-in-water nanoemulsion produced from *Pereskia aculeata* Miller mucilage. *Ultrasonics Sonochemistry*, 50(July 2018), 339–353. <https://doi.org/10.1016/j.ultsonch.2018.09.036>
- Lago, C. C., & Noreña, C. P. Z. (2015). Thermodynamic analysis of sorption isotherms of dehydrated yacon (*Smallanthus sonchifolius*) bagasse. *Food Bioscience*, 12, 26–33. <https://doi.org/10.1016/j.fbio.2015.07.001>

- Liébanes, M. D., Aragón, J. M., Palancar, M. C., Arévalo, G., & Jiménez, D. (2006). Equilibrium moisture isotherms of two-phase solid olive oil by-products: Adsorption process thermodynamics. *Colloids and Surfaces A: Physicochemical and Engineering Aspects*, 282–283, 298–306. <https://doi.org/10.1016/j.colsurfa.2006.03.025>
- Lima Junior, F. A., Conceição, M. C., Resende, J. V. de, Junqueira, L. A., Pereira, C. G., & Prado, M. E. T. (2013). Response surface methodology for optimization of the mucilage extraction process from *Pereskia aculeata* Miller. *Food Hydrocolloids*, 33(1), 38–47. <https://doi.org/10.1016/j.foodhyd.2013.02.012>
- Martin, A. A., de Freitas, R. A., Sasaki, G. L., Evangelista, P. H. L., & Sierakowski, M. R. (2017). Chemical structure and physical-chemical properties of mucilage from the leaves of *Pereskia aculeata*. *Food Hydrocolloids*, 70, 20–28. <https://doi.org/10.1016/j.foodhyd.2017.03.020>
- McMinn, W. A. M., Al-Muhtaseb, A. H., & Magee, T. R. A. (2004). Moisture sorption characteristics of starch gels. part II: Thermodynamic properties. *Journal of Food Process Engineering*, 27(3), 213–227. <https://doi.org/10.1111/j.1745-4530.2004.tb00631.x>
- McMinn, W. A. M., & Magee, T. R. A. (2003). Thermodynamic properties of moisture sorption of potato. *Journal of Food Engineering*, 60(2), 157–165. [https://doi.org/10.1016/S0260-8774\(03\)00036-0](https://doi.org/10.1016/S0260-8774(03)00036-0)
- Mercê, A. L. R., Landaluze, J. S., Mangrich, A. S., Szpoganicz, B., & Sierakowski, M. R. (2000). Complexes of arabinogalactan of *Pereskia aculeata* and  $\text{Co}^{2+}$ ,  $\text{Cu}^{2+}$ ,  $\text{Mn}^{2+}$ , and  $\text{Ni}^{2+}$ . *Bioresource Technology*. [https://doi.org/10.1016/S0960-8524\(00\)00078-X](https://doi.org/10.1016/S0960-8524(00)00078-X)
- Monte, M. L., Moreno, M. L., Senna, J., Arrieche, L. S., & Pinto, L. A. A. (2018). Food bioscience moisture sorption isotherms of chitosan-glycerol films: Thermodynamic properties and microstructure. 22(February), 170–177.
- Moreira, R., Chenlo, F., Torres, M. D., & Vallejo, N. (2008). Thermodynamic analysis of experimental sorption isotherms of loquat and quince fruits. *Journal of Food Engineering*, 88(4), 514–521. <https://doi.org/10.1016/j.jfoodeng.2008.03.011>
- Mrad, N. D., Bonazzi, C., Boudhrioua, N., Kechaou, N., & Courtois, F. (2012). Moisture sorption isotherms, thermodynamic properties, and glass transition of pears and apples. *Drying Technology*, 30(13), 1397–1406. <https://doi.org/10.1080/07373937.2012.683843>
- Oliveira, N. L., Rodrigues, A. A., Oliveira Neves, I. C., Teixeira Lago, A. M., Borges, S. V., & de Resende, J. V. (2019). Development and characterization of biodegradable films based on *Pereskia aculeata* Miller mucilage. *Industrial Crops and Products*, 130(August 2018), 499–510. <https://doi.org/10.1016/j.indcrop.2019.01.014>
- Othmer, D. F. (1940). Correlating Vapor Pressure and Latent Heat Data A NEW PLOT. 32, 841–856.
- Pérez-Alonso, C., Beristain, C. I., Lobato-Calleros, C., Rodríguez-Huezo, M. E., & Vernon-Carter, E. J. (2006). Thermodynamic analysis of the sorption isotherms of pure and blended carbohydrate polymers. *Journal of Food Engineering*, 77(4), 753–760. <https://doi.org/10.1016/j.jfoodeng.2005.08.002>
- Rizvi, S. S. H., & Benado, A. L. (1983). Thermodynamic Analysis of Drying Foods. *Drying Technology*, 2(4), 471–502. <https://doi.org/10.1080/07373938408959849>
- Sánchez-Sáenz, E. O., Pérez-Alonso, C., Cruz-Olivares, J., Román-Guerrero, A., Baéz-González, J. G., & Rodríguez-Huezo, M. E. (2011). Establishing the most suitable storage conditions for microencapsulated allspice essential oil entrapped in blended biopolymers matrices. *Drying Technology*, 29(8), 863–872. <https://doi.org/10.1080/07373937.2010.545495>
- Schneider, A. S. (1981). Hydration of biological membranes. Em L. B. Rockland & G. F. Stewart (Orgs.), *Water activity: Influences on food quality* (p. 377–405). Academic Press.

- Silva, E. K., Fernandes, R. V. de B., Borges, S. V., Botrel, D. A., & Queiroz, F. (2014). Water adsorption in rosemary essential oil microparticles: Kinetics, thermodynamics and storage conditions. *Journal of Food Engineering*, 140, 39–45. <https://doi.org/10.1016/j.jfoodeng.2014.05.003>
- Suppakul, P., Chalernsook, B., Ratisuthawat, B., Prapasitthi, S., & Munchukangwan, N. (2013). Empirical modeling of moisture sorption characteristics and mechanical and barrier properties of cassava flour film and their relation to plasticizing–antiplasticizing effects. *LWT - Food Science and Technology*, 50(1), 290–297. <https://doi.org/10.1016/j.lwt.2012.05.013>
- Takeiti, C. Y., Antonio, G. C., Motta, E. M. P., Fernanda, P., Park, K. J., Takeiti, C. Y., Antonio, G. C., Motta, E. M. P., & Fernanda, P. (2009). Nutritive evaluation of a non-conventional leafy vegetable (*Pereskia aculeata* Miller). 7486. <https://doi.org/10.1080/09637480802534509>
- Tunç, S., & Duman, O. (2007). Thermodynamic properties and moisture adsorption isotherms of cottonseed protein isolate and different forms of cottonseed samples. *Journal of Food Engineering*. <https://doi.org/10.1016/j.jfoodeng.2006.10.015>
- Velázquez-Gutiérrez, S. K., Figueira, A. C., Rodríguez-Huezo, M. E., Román-Guerrero, A., Carrillo-Navas, H., & Pérez-Alonso, C. (2015). Sorption isotherms, thermodynamic properties and glass transition temperature of mucilage extracted from chia seeds (*Salvia hispanica* L.). *Carbohydrate Polymers*, 121, 411–419. <https://doi.org/10.1016/j.carbpol.2014.11.068>
- Viganó, J., Azuara, E., Telis, V. R. N., Beristain, C. I., Jiménez, M., & Telis-Romero, J. (2012). Role of enthalpy and entropy in moisture sorption behavior of pineapple pulp powder produced by different drying methods. *Thermochimica Acta*, 528, 63–71. <https://doi.org/10.1016/j.tca.2011.11.011>
- Wexler, A. (1976). Vapor pressure formulation for water in range 0 to 100 C. A revision. *Journal of Research of the National Bureau of Standards Section A: Physics and Chemistry*, 80A(5–6), 775–785. <https://doi.org/10.6028/jres.080A.071>